CHEMISTRY

Asymmetric photon transport in organic semiconductor nanowires through electrically controlled exciton diffusion

Qiu Hong Cui,[1] Qian Peng,[1] Yi Luo,[2]* Yuqian Jiang,[3] Yongli Yan,[1] Cong Wei,[1] Zhigang Shuai,[3] Cheng Sun,[4] Jiannian Yao,[1] Yong Sheng Zhao[1]*

The ability to steer the flow of light toward desired propagation directions is critically important for the realization of key functionalities in optical communication and information processing. Although various schemes have been proposed for this purpose, the lack of capability to incorporate an external electric field to effectively tune the light propagation has severely limited the on-chip integration of photonics and electronics. Because of the noninteractive nature of photons, it is only possible to electrically control the flow of light by modifying the refractive index of materials through the electro-optic effect. However, the weak optical effects need to be strongly amplified for practical applications in high-density photonic integrations. We show a new strategy that takes advantage of the strong exciton-photon coupling in active waveguides to effectively manipulate photon transport by controlling the interaction between excitons and the external electric field. Single-crystal organic semiconductor nanowires were used to generate highly stable Frenkel exciton polaritons with strong binding and diffusion abilities. By making use of directional exciton diffusion in an external electric field, we have realized an electrically driven asymmetric photon transport and thus directional light propagation in a single nanowire. With this new concept, we constructed a dual-output single wire–based device to build an electrically controlled single-pole double-throw optical switch with fast temporal response and high switching frequency. Our findings may lead to the innovation of concepts and device architectures for optical information processing.

INTRODUCTION

Breaking the symmetry of photon transport is essential for the construction of optical diodes or isolators in photonic integrated circuits (*1*–*7*), which, in many ways, resemble the roles played by semiconductor *p*-*n* junctions on electronic chips. A series of photonic schemes have been used to achieve asymmetric light propagation based on magneto-optical (*8*), topological photonics (*9*, *10*) or optical nonlinearity (*11*) by exploiting the asymmetric coupling efficiency or propagation loss along the two opposite directions of light propagation. Unfortunately, the inherent complexity in the device configuration and large footprints restrict their applications in integrated photonics. In contrast, controlling the photon flows with a static electric field offers a much attractive solution, because with it, the functions of integrated photonic devices will be broadly expanded because of the higher tunability and higher compatibility with electronics (*12*, *13*). However, this is fundamentally difficult because photons, being chargeless and massless gauge bosons, barely interact with one another nor do they respond to the external stimuli.

On the other hand, in an active semiconductor waveguide, photons can be coupled with excitons to form a new type of hybrid state known as exciton polariton (EP) (*14*–*17*). These mixed light-matter quasiparticles can propagate along the waveguide and subsequently couple out to restore their original form as photons. Thus, whereas EPs are capable of carrying photons, they also exhibit charged electron/hole characteristics (inherited from their excitonic components) (*18*), which can be manipulated using external electric fields (*19*). In particular, the directional exciton diffusion has been experimentally realized by locally applying an electric field (*20*–*22*) or acoustic field (*23*) on an asymmetric quantum well structure, but the asymmetric exciton diffusion has never been exploited for the realization of electrically controlled directional light propagation.

[1]Institute of Chemistry, Chinese Academy of Sciences, Beijing 100190, China. [2]Hefei National Laboratory for Physical Sciences at the Microscale and Synergetic Innovation Center of Quantum Information and Quantum Physics, University of Science and Technology of China, Hefei, Anhui 230026, China. [3]Key Laboratory of Organic Optoelectronics and Molecular Engineering, Department of Chemistry, Tsinghua University, Beijing 100084, China. [4]Department of Mechanical Engineering, Northwestern University, Evanston, IL 60208–3109, USA.
*Corresponding author. Email: yszhao@iccas.ac.cn (Y.S.Z.); yiluo@ustc.edu.cn (Y.L.)

RESULTS

Organic semiconductor nanowires for asymmetric exciton diffusion

The fact that the external electric field may reduce the stability of the exciton indicates that the effective control of light propagation can only be achieved for systems with large exciton binding energy. In this context, the Frenkel-type exciton in organic semiconductors is particularly attractive, owing to its high binding energy and long diffusion path length. The generated polaritons in highly ordered organic crystals are known to be highly stable even at room temperature (*24*, *25*) and can propagate up to a millimeter (*26*). In an organic single crystal, the uniform distributions of generated excitons in space often result in the omnidirectional exciton diffusion. In principle, one can generate uneven spatial distribution of excitons by using sophisticated structural design to achieve the asymmetric diffusion but at the expense of very complicated fabrication procedures. We believe that the utilization of an external electric field can reach the same goal without facing these difficulties. It is known that the interaction between the external electric field and an exciton can produce an external interaction potential, $V_{ext} = -\boldsymbol{\mu}_e \cdot \boldsymbol{E}$, where $\boldsymbol{\mu}_e$ is the transition moment of the exciton and $\boldsymbol{E}$ is the external field. Such a directional interaction can break the otherwise symmetric distribution of the excitons and thus results in a directional light propagation mediated via the formation of EPs.

Here, we present a successful demonstration of the asymmetric photon transport and thus directional light propagation in one-dimensional

nanocrystals constructed from the organic semiconductor compound 9,10-bis(phenylethynyl)anthracene (BPEA; fig. S1). The highly symmetric structure of BPEA helped to fabricate the crystalline wires. The choice of BPEA was further motivated by its high absorption/emission efficiency, outstanding optical waveguiding performance (*27*), and large exciton binding energy (652 meV; see section S1). Moreover, the high symmetry of BPEA molecule can also effectively minimize the negative Stark effects on its large exciton diffusion length. BPEA nanowires of high monodispersity (fig. S2) were fabricated with a physical vapor transport technique (see section S2). The BPEA nanowires show very similar absorption and photoluminescence spectra to those of the BPEA powder (fig. S3), which indicates that the BPEA does not undergo chemical reaction during the vapor transportation. An atomic force microscopy (AFM) image (fig. S4) confirmed that the wires have very smooth surfaces and rectangular cross section. An x-ray diffraction (XRD) pattern taken for the nanowires (fig. S5) verified the high crystallinity of the nanowires, which can be indexed to the monoclinic phase. A transmission electron microscopy (TEM) image of a typical wire and corresponding selected-area electron diffraction (SAED) patterns are shown in Fig. 1A and fig. S6, which show that the prepared wires have a close-packed crystalline structure with smooth surfaces growing along the [010] direction. The thermodynamically stable morphology of BPEA demonstrates cofacial herringbone one-dimensional π stacking of the conjugated molecules along the *b* axis [Fig. 1A (inset) and fig. S7]. The intermolecular distance along the stacking direction is as short as 3.37 Å, which results in a large overlap between adjacent π orbitals and further improves the migration of excitons (*28*, *29*) and the exciton-photon coupling.

The photoluminescence image of the wires in Fig. 1B exhibits orange emission, with bright spots at the wire tips, under ultraviolet excitation. This active waveguiding characteristic indicates that the photoluminescence energy can propagate along the wire axis. The guided-light intensity has much slower decay at longer wavelengths (Fig. 1C and fig. S8), and the complex refractive index shows strong dispersion in high photon energy bands (fig. S8), which clearly indicate the formation of EPs following excitation (*30*, *31*). It can be seen that the emission at both ends has almost identical intensity (Fig. 1C and fig. S9) when the ultraviolet excitation is located in the middle of the nanowire. This indicates that the EPs in the waveguide can transfer freely in the two opposite directions with equal probability, and the density of the exciton is symmetrically distributed in space in this system. The introduction of the external electric field on the system can thus change the density distribution of the exciton through the alternation of the interaction potential (*32*–*34*), resulting in the intensity difference of the emissions from the two ends, as schematically shown in Fig. 1D.

Realization and modulation of electrically controlled asymmetric photon transport

A simple experimental setup to verify the effects of the electric field involves placing the electric field coplanar with the long wire axis, as illustrated in Fig. 2A and fig. S10. When the excitation is located at one end, the forward and backward transport of EPs with respect to the direction of the electric field should be drastically different, leading to asymmetric light propagation. This is exactly what we have found from our experiments, in which two parallel electrodes with constant channel width are placed close to each side of a typical nanowire to establish a

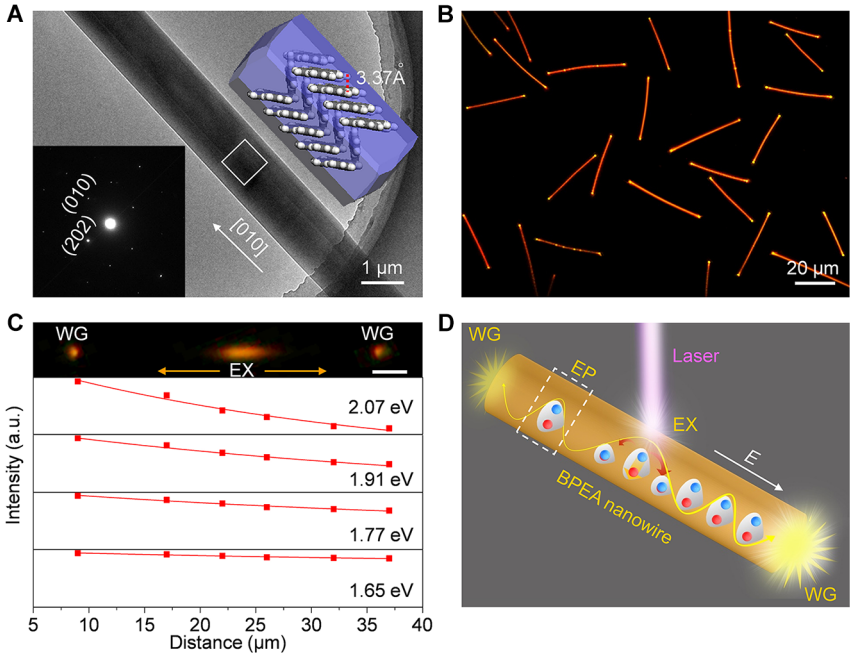

Fig. 1. EP propagation in BPEA nanowires for asymmetric photon transport. (**A**) TEM image of a single BPEA wire. Insets: SAED pattern (left) collected from the microarea marked with a white square and the thermodynamically stable molecular stacking in the crystal nanowire (right). The packing arrangement of molecules is along the *b* axis with the shortest intermolecular distance of 3.37 Å, which improves the migration of excitons and the exciton-photon coupling. (**B**) Photoluminescence image of the BPEA nanowires under ultraviolet (330 to 380 nm) excitation. (**C**) Microarea photoluminescence image of a typical wire locally excited from the middle and guided distance-dependent photoluminescence intensities at different wavelengths. The photoluminescence spectra were collected from the left tip of the wire by accurately shifting the excitation laser spot. EX, excited spot; WG, waveguided emission; a.u., arbitrary units. (**D**) Schematic depiction of the asymmetric light propagation under an electric field. The electrically induced asymmetric EP migration results in a stronger outcoupling along the field compared with that against the field.

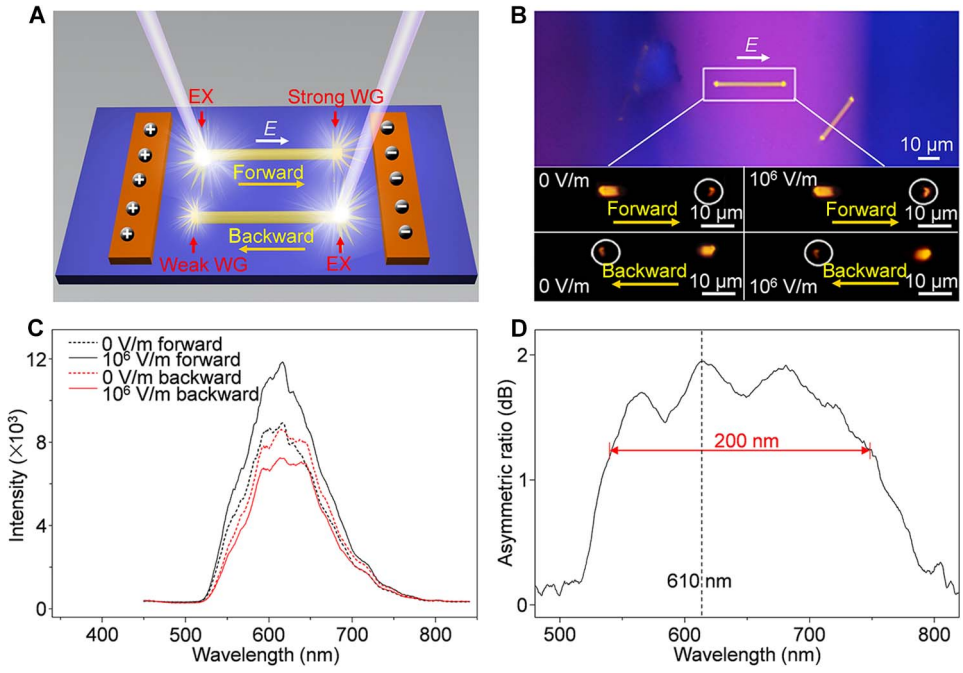

Fig. 2. Realization of asymmetric photon transport. (**A**) Schematic depiction of the device configuration. The field is applied in-plane with the light propagation to provide an efficient way for asymmetric power coupling to the waveguides. The nanowire was successively excited from one end, and the outcoupled light was collected from the opposite end. When the excitation beam is focused at one end, EPs would propagate forward and backward with respect to the direction of the electric field along the wire axis. (**B**) Photoluminescence microscopy image of the device and a typical wire for the optical measurements. The white circles mark the outcoupled emissions from the wire tip without and with forward and backward electric fields (1.0×10^6 V/m), respectively, which indicates that the forward propagation of the waveguided emission along the field increases, and the backward propagation decreases in comparison with that in the absence of the field. (**C**) Corresponding outcoupled emission spectra collected from the tips of the wire (~34 μm) under applied fields of 0 and 1.0×10^6 V/m (forward and backward). (**D**) Plot of asymmetric ratio versus wavelength, which shows a good photon transport asymmetry over a large wavelength bandwidth (>200 nm).

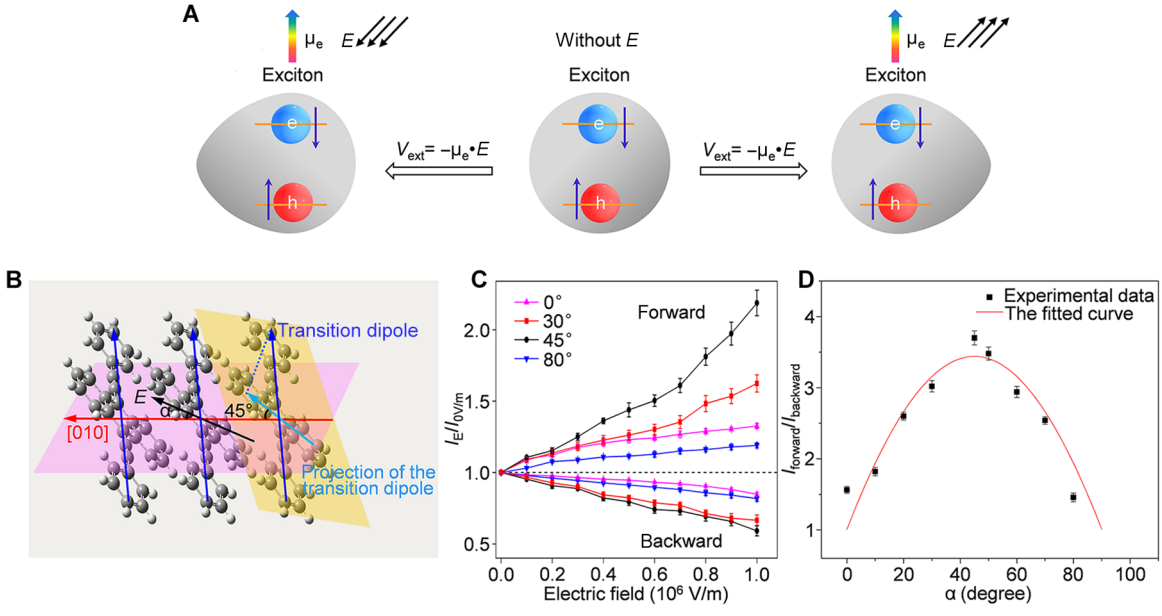

Fig. 3. Principle and modulation of the asymmetric photon transport. (**A**) Schematic of the exciton diffusion in the absence and presence of an external electric field. With respect to the exciton diffusion without the electric field effect, the applied electric field would alter the exciton diffusion ability through the extra interaction potential $V_{ext} = -\boldsymbol{\mu}_e \cdot \boldsymbol{E}$, resulting in the increase or decrease in the local potential. (**B**) Schematic depiction of the spatial relationship between BPEA molecular transition dipole moment (blue arrows) and the growth direction (red arrow) of the nanowire. The projection of the transition dipole (light blue arrow) leans at an angle of 45° to the long wire axis. (**C**) Plots of forward and backward photoluminescence intensity modulations at 610 nm versus α. (**D**) $I_{forward}/I_{backward}$ versus α at an electric field strength of 1.0×10^6 V/m. The line is fitted with the $\cos(\alpha - 45°)$ function. Error bars represent the SD of three representative measurements.

coplanar relationship between the electric field and the light propagation (Fig. 2B). Compared with the guided photoluminescence spot in the absence of a field, the forward transport at 1.0×10^6 V/m gives a larger and brighter light spot, contrasting sharply with the small and obscure one at the backward output end. The corresponding outcoupled spectra in Fig. 2C quantitatively show the contrast in the intensity of the optical signal for forward and backward propagations under the electric field, suggesting that much higher propagation efficiency is achieved when the EPs propagate along the field direction. The plot of the asymmetric ratio [$AR = 10 \times \lg(I_{forward}/I_{backward})$] versus wavelength in the inset to Fig. 2D demonstrates a strong propagation asymmetry, with asymmetric ratios larger than 1.2 dB, over a bandwidth of 200 nm and a maximum value of 1.9 dB at 610 nm.

The convincing experimental evidence of the asymmetric optical outcoupling indicates that our proposed strategy of using external electric field to control the diffusion of excitons works well in the organic nanowires. To further demonstrate the basic working principle, we have carried out a model calculation to describe the exciton diffusion under the external electric field (fig. S11). The occurrence of the interaction potential, V_{ext}, can produce a directional force on the exciton and can cause an asymmetric redistribution of the exciton density (Fig. 3A), as reflected by an extra field-dependent term in the diffusion equation. The calculated results clearly demonstrate the huge effects of the external field on the asymmetric exciton diffusion. As a comparison experiment, it is found that the electric field has negligible effects on the passively guided light without generation of excitons under

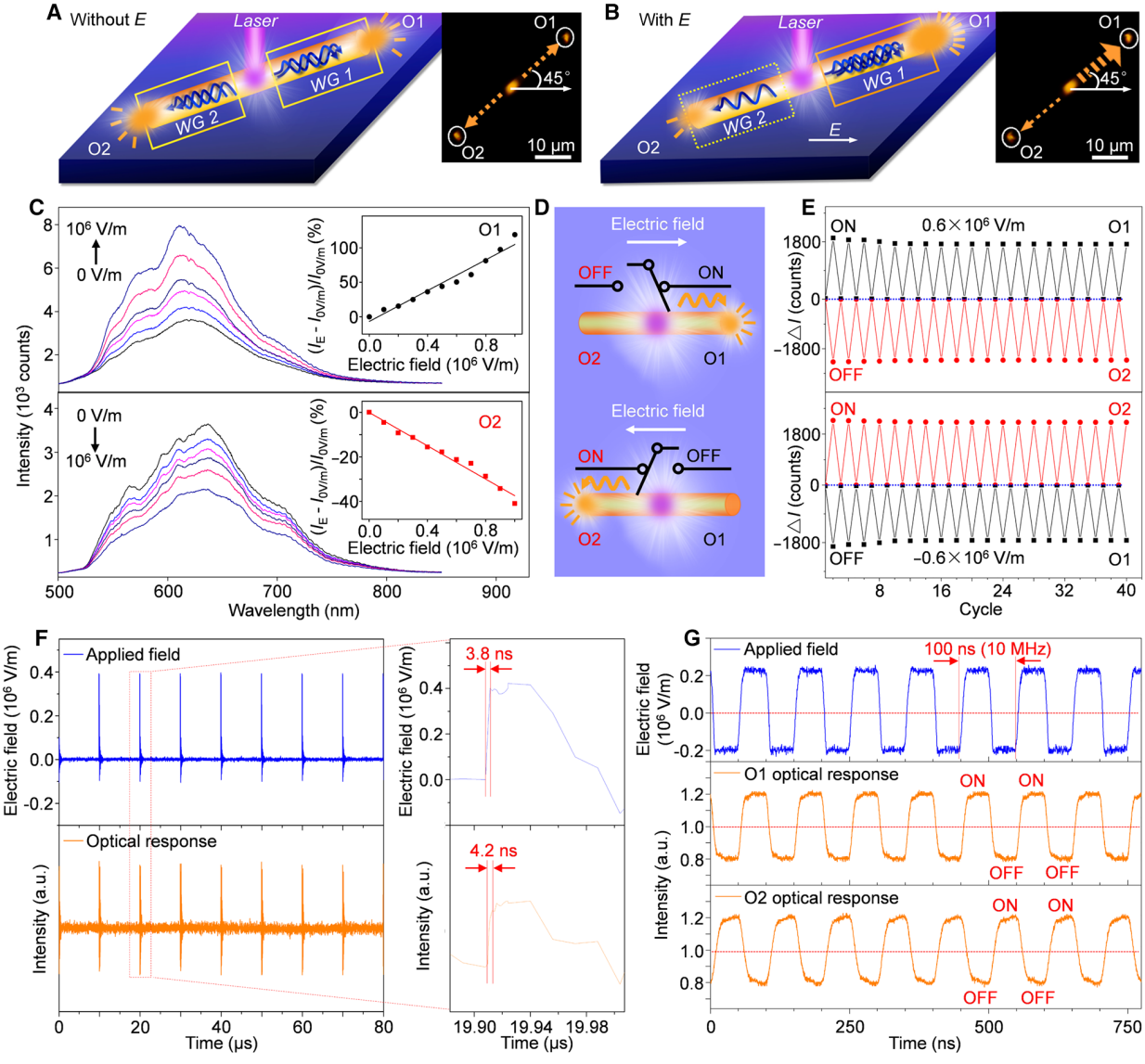

Fig. 4. Design and realization of SPDT optical switch based on the asymmetric photon transport. (**A** and **B**) Configurations of a dual-output device in the absence (A) and presence (B) of an electric field. Insets: Photoluminescence images of a wire with $\alpha = 45°$. The two tips (marked with white circles) are monitored as the output ports O1 and O2. WG, waveguide. (**C**) Outcoupled spectra of O1 and O2 under different field strengths ranging from 0 to 1.0×10^6 V/m. Insets: Linear fits of the outcoupling modulation from ports O1 and O2 versus the electric field strength. (**D**) Schematic illustration of the SPDT optical switches that can be controlled by operating the electric field. (**E**) Cyclic on/off switching behavior, which is changed by repeatedly altering the direction of electric field. (**F**) Series of light pulses with response time of 4.2 ns generated by electrical pulses with a rise time of 3.8 ns. (**G**) Temporal intensity profiles of O1 and O2 with 10-MHz electrical pulses.

the excitation of a 635-nm laser (fig. S12), which further confirms that the asymmetric photon transport results from the response of the EPs, rather than the electro-optic effect on the refraction index.

Within this interactive picture, the asymmetric optical outcoupling can be modulated by varying the field strength and field direction, as the corresponding exciton diffusion ability is determined by the interaction potential that is related both to the strength of the field and to the angle between the molecular transition dipole and the electric field, θ. It can be seen from Fig. 3B that the BPEA transition dipole leans an angle of 45° to the growth direction of the nanowires (also see figs. S13 and S14) (*35*). As shown in Fig. 3C, the opposite intensity modulations in the two opposing directions are both quasi-linearly amplified on increasing the electric field strength *E*. Moreover, various field effects are observed under different angles α between the electric field and the long axis of the nanowire. It is found that the relationship between $I_{forward}/I_{backward}$ and the angle at 1.0×10^6 V/m (Fig. 3D) can be described by cos(α − 45°), and the maximum asymmetric ratio up to 5 dB can be achieved at α = 45°. All these experimental evidences clearly demonstrate that the photon transport asymmetry in organic molecular crystals can be effectively tuned by the electric field through the control of the exciton diffusion ability.

Electrically controlled single-pole double-throw optical switch

The asymmetric light propagation realized with directional exciton diffusion in the composition-homogeneous nanocrystals facilitates the fabrication of nanowire-based photonic devices. For instance, a single nanowire with dual waveguide output might behave as a connection of two unidirectional waveguides when the laser is focused on the middle of the wire (Fig. 4A). According to the obtained angular dependence of propagation asymmetry, the wire with α = 45° was selected for optimal operation. Because of the reverse direction of light propagation, the outcoupled light intensities of output 1 (O1) and output 2 (O2) undergo opposite effects under the electric field (Fig. 4B). The variable asymmetric output can be achieved by changing the input electric field, as shown in Fig. 4C. The modulation ratios $[(I_E - I_{0V/m})/I_{0V/m}]$ of two wire tips scale linearly as a function of the applied field strength and can be deduced from the fitting equation for O1 and O2, respectively: $I_{O1} = (1.11 \times 10^{-6}E + 1.0)\, I_{0V/m}$ and $I_{O2} = (-3.73 \times 10^{-7}E + 1.0)\, I_{0V/m}$. This dual-output device enables the continuous distribution of the output optical signals in one channel and further allows us to design an electrically controlled single-pole double-throw (SPDT) optical switch (Fig. 4D). When a constant field with the strength of 0.6×10^6 V/m is applied on the device, the output of O1 increases, which is defined as the "on" state. Meanwhile, the outcoupling of O2 decreases, corresponding to the "off" state. On the basis of the field-controlled exciton diffusion, the on and off states of two outputs can be interchanged by reversing the field direction, as shown in Fig. 4E. The relative intensities for all 20 cycles remain almost the same, demonstrating the stable switching behavior with low device fatigue.

For such an electric field–controlled optical switch, the switching speed and frequency should naturally be determined by the performance of the applied electric instrument. We carried out measurements using a nanosecond electric pulse generator. One can immediately observe that the optical response of the switch is always the same as the response of the pulse generator. More specifically, our SPDT switch reaches a high switching speed of 4.2 ns with an electric field speed of 3.8 ns (Fig. 4F and fig. S15) and a frequency of 10 MHz under the 10-MHz electric pulses (Fig. 4G). By further optimizing the electric instrument, the frequency of our SPDT switch can always be enlarged (fig. S16).

DISCUSSION

In conclusion, asymmetric photon transport has been realized in single-crystalline organic nanowire waveguides as a result of electrically controlling the directional exciton diffusion during the active light guiding. Electrotunable asymmetric optical outcoupling was achieved and maximized by altering the field strength and direction. Furthermore, an electrically controlled high-speed SPDT optical switch has been constructed on a single nanowire. These results provide insight into the design of nonreciprocal photonic nanodevices and will promote the advancement of exciton-based optical elements toward miniaturized photonic circuits and on-chip integration of photonics and electronics.

MATERIALS AND METHODS

Nanowire synthesis

BPEA nanowire crystals were obtained using a physical vapor transport technique. The experimental procedure is described in detail in section S2.

Device fabrication

The BPEA nanowires were deposited directly onto a Si/SiO_2 substrate, and two rectangular Cu electrodes were then attached with a fixed channel width of 100 μm to incorporate several BPEA wires with different angles α in between. The thickness of electrodes (on the millimeter scale) ensured the application of a uniform electric field in the plane of the wires. The wires and electrodes formed a nonintimate contact with each other to prevent the charge injections that might bring detrimental effects to the device. The structure of the device is illustrated in fig. S10.

Optical characterization

The optical measurements were performed on a home-built confocal microphotoluminescence system (fig. S17). A single wire was locally excited with a 351-nm laser beam (BeamLok 2065, Spectra-Physics) focused by an objective lens (50×; numerical aperture, 0.8; Nikon CFLU Plan). The emission of the wire was selectively collected from the tip using a confocal microscopy setup with a 1-μm pinhole. The light was subsequently coupled to a grating spectrometer (Acton SP2300) with a matched thermal electrically cooled charge-coupled device (ProEm: 1600 × 200B, Princeton Instruments).

For the measurements of electric field–induced asymmetric light propagation, an external electric field was applied with a commercial dc voltage supplier. The pulsed electric field was applied using a nanosecond signal generator, which supports tunable amplitude, frequency, and rise time (fig. S18). The optical signals were detected using a silicon photodetector and monitored using an oscilloscope to obtain the response time and switching frequency of the switch.

SUPPLEMENTARY MATERIALS

Supplementary material for this article is available at http://advances.sciencemag.org/cgi/content/full/4/3/eaap9861/DC1

section S1. Calculation of BPEA excitons

section S2. Preparation and structural characterization of BPEA nanowires

section S3. Formation of EPs in the BPEA nanowires

section S4. Structure of the device

REFERENCES AND NOTES

1. L. Fan, J. Wang, L. T. Varghese, H. Shen, B. Niu, Y. Xuan, A. M. Weiner, M. Qi, An all-silicon passive optical diode. *Science* **335**, 447–450 (2012).
2. A. Regensburger, C. Bersch, M.-A. Miri, G. Onishchukov, D. N. Christodoulides, U. Peschel, Parity-time synthetic photonic lattices. *Nature* **488**, 167–171 (2012).
3. X. Yin, X. Zhang, Unidirectional light propagation at exceptional points. *Nat. Mater.* **12**, 175–177 (2013).
4. D. Jalas, A. Petrov, M. Eich, W. Freude, S. Fan, Z. Yu, R. Baets, M. Popović, A. Melloni, J. D. Joannopoulos, M. Vanwolleghem, C. R. Doerr, H. Renner, What is—and what is not—an optical isolator. *Nat. Photonics* **11**, 579–582 (2013).
5. L. Feng, Y.-L. Xu, W. S. Fegadolli, M.-H. Lu, J. E. B. Oliveira, V. R. Almeida, Y.-F. Chen, A. Scherer, Experimental demonstration of a unidirectional reflectionless parity-time metamaterial at optical frequencies. *Nat. Mater.* **12**, 108–113 (2013).
6. J. Petersen, J. Volz, A. Rauschenbeutel, Chiral nanophotonic waveguide interface based on spin-orbit interaction of light. *Science* **346**, 67–71 (2014).
7. K. Fang, S. Fan, Controlling the flow of light using the inhomogeneous effective gauge field that emerges from dynamic modulation. *Phys. Rev. Lett.* **111**, 203901 (2013).
8. S. Sugano, N. Kojima, *Magneto-optics* (Springer, 2000).
9. L. Lu, J. D. Joannopoulos, M. Soljačić, Topological photonics. *Nat. Photonics* **8**, 821–829 (2014).
10. M. Hafezi, S. Mittal, J. Fan, A. Migdall, J. M. Taylor, Imaging topological edge states in silicon photonics. *Nat. Photonics* **7**, 1001–1005 (2013).
11. K. Gallo, G. Assanto, K. R. Parameswaran, M. M. Fejer, All-optical diode in a periodically poled lithium niobate waveguide. *Appl. Phys. Lett.* **79**, 314–316 (2001).
12. A. Davoyan, N. Engheta, Electrically controlled one-way photon flow in plasmonic nanostructures. *Nat. Commun.* **5**, 5250 (2014).
13. A. B. Greytak, C. J. Barrelet, Y. Li, C. M. Lieber, Semiconductor nanowire laser and nanowire waveguide electro-optic modulators. *Appl. Phys. Lett.* **87**, 151103 (2005).
14. P. M. Walker, L. Tinkler, M. Durska, D. M. Whittaker, I. J. Luxmoore, B. Royall, D. N. Krizhanovskii, M. S. Skolnick, I. Farrer, D. A. Ritchie, Exciton polaritons in semiconductor waveguides. *Appl. Phys. Lett.* **102**, 012109 (2013).
15. T. Ellenbogen, K. B. Crozier, Exciton-polariton emission from organic semiconductor optical waveguides. *Phys. Rev. B* **84**, 161304(R) (2011).
16. L. K. van Vugt, S. Rühle, P. Ravindran, H. C. Gerritsen, L. Kuipers, D. Vanmaekelbergh, Exciton polaritons confined in a ZnO nanowire cavity. *Phys. Rev. Lett.* **97**, 147401 (2006).
17. H. M. Gibbs, G. Khitrova, S. W. Koch, Exciton-polariton light-semiconductor coupling effects. *Nat. Photonics* **5**, 275–282 (2011).
18. S. Kéna-Cohen, S. R. Forrest, Room-temperature polariton lasing in an organic single-crystal microcavity. *Nat. Photonics* **4**, 371–375 (2010).
19. T. Katsuyama, K. Ogawa, Excitonic polaritons in quantum-confined systems and applications to optoelectronic devices. *J. Appl. Phys.* **75**, 7607–7625 (1994).
20. A. A. High, E. E. Novitskaya, L. V. Butov, M. Hanson, A. C. Gossard, Control of exciton fluxes in an excitonic integrated circuit. *Science* **321**, 229–231 (2008).
21. M. Hagn, A. Zrenner, G. Böhm, G. Weimann, Electric-field-induced exciton transport in coupled quantum well structures. *Appl. Phys. Lett.* **67**, 232 (1995).
22. A. A. High, A. T. Hammack, L. V. Butov, M. Hanson, A. C. Gossard, Exciton optoelectronic transistor. *Opt. Lett.* **32**, 2466–2468 (2007).
23. A. Violante, K. Cohen, S. Lazić, R. Hey, R. Rapaport, P. V. Santos, Dynamics of indirect exciton transport by moving acoustic fields. *New J. Phys.* **16**, 033035 (2014).
24. D. G. Lidzey, D. D. C. Bradley, M. S. Skolnick, T. Virgili, S. Walker, D. M. Whittaker, Strong exciton-photon coupling in an organic semiconductor microcavity. *Nature* **395**, 53–55 (1998).
25. D. G. Lidzey, D. D. C. Bradley, A. Armitage, S. Walker, M. S. Skolnick, Photon-mediated hybridization of Frenkel excitons in organic semiconductor microcavities. *Science* **288**, 1620–1623 (2000).
26. K. Takazawa, J.-i. Inoue, K. Mitsuishi, T. Takamasu, Fraction of a millimeter propagation of exciton polaritons in photoexcited nanofibers of organic dye. *Phys. Rev. Lett.* **105**, 067401 (2010).
27. Y. S. Zhao, J. Xu, A. Peng, H. Fu, Y. Ma, L. Jiang, J. Yao, Optical waveguide based on crystalline organic microtubes and microrods. *Angew. Chem. Int. Ed.* **47**, 7301–7305 (2008).
28. R. R. Lunt, J. B. Benziger, S. R. Forrest, Relationship between crystalline order and exciton diffusion length in molecular organic semiconductors. *Adv. Mater.* **22**, 1233–1236 (2010).
29. D. Chaudhuri, D. Li, Y. Che, E. Shafran, J. M. Gerton, L. Zang, J. M. Lupton, Enhancing long-range exciton guiding in molecular nanowires by H-aggregation lifetime engineering. *Nano Lett.* **11**, 488–492 (2011).
30. L. K. van Vugt, B. Piccione, C.-H. Cho, P. Nukala, R. Agarwal, One-dimensional polaritons with size-tunable and enhanced coupling strengths in semiconductor nanowires. *Proc. Natl. Acad. Sci. U.S.A.* **108**, 10050–10055 (2011).
31. C. Zhang, C.-L. Zou, Y. Yan, R. Hao, F.-W. Sun, Z.-F. Han, Y. S. Zhao, J. Yao, Two-photon pumped lasing in single-crystal organic nanowire exciton polariton resonators. *J. Am. Chem. Soc.* **133**, 7276–7279 (2011).
32. J. A. Schuller, S. Karaveli, T. Schiros, K. He, S. Yang, I. Kymissis, J. Shan, R. Zia, Orientation of luminescent excitons in layered nanomaterials. *Nat. Nanotechnol.* **8**, 271–276 (2013).
33. T. C. H. Liew, A. V. Kavokin, T. Ostatnický, M. Kaliteevski, I. A. Shelykh, R. A. Abram, Exciton-polariton integrated circuits. *Phys. Rev. B* **82**, 033302 (2010).
34. K. Ogawa, T. Katsuyama, M. Kawata, Electric field dependence of the propagation of quantum-well exciton polaritons in a waveguide structure. *Phys. Rev. B* **46**, 13289 (1992).
35. Y. Yan, C. Zhang, J. Y. Zheng, J. Yao, Y. S. Zhao, Optical modulation based on direct photon-plasmon coupling in organic/metal nanowire heterojunctions. *Adv. Mater.* **24**, 5681–5686 (2012).
36. S. F. Alvarado, P. F. Seidler, D. G. Lidzey, D. D. C. Bradley, Direct determination of the exciton binding energy of conjugated polymers using a scanning tunneling microscope. *Phys. Rev. Lett.* **81**, 1082 (1998).
37. P. K. Nayak, N. Periasamy, Calculation of electron affinity, ionization potential, transport gap, optical band gap and exciton binding energy of organic solids using 'solvation' model and DFT. *Org. Electron.* **10**, 1396–1400 (2009).
38. H. Najafov, B. Lee, Q. Zhou, L. C. Feldman, V. Podzorov, Observation of long-range exciton diffusion in highly ordered organic semiconductors. *Nat. Mater.* **9**, 938–943 (2010).
39. R. R. Lunt, N. C. Giebink, A. A. Belak, J. B. Benziger, S. R. Forrest, Exciton diffusion lengths of organic semiconductor thin films measured by spectrally resolved photoluminescence quenching. *J. Appl. Phys.* **105**, 053711 (2009).
40. M. Law, D. J. Sirbuly, J. C. Johnson, J. Goldberger, R. J. Saykally, P. Yang, Nanoribbon waveguides for subwavelength photonics integration. *Science* **305**, 1269–1273 (2004).
41. D. O'Carroll, I. Lieberwirth, G. Redmond, Microcavity effects and optically pumped lasing in single conjugated polymer nanowires. *Nat. Nanotechnol.* **2**, 180–184 (2007).
42. B. Piccione, L. K. van Vugt, R. Agarwal, Propagation loss spectroscopy on single nanowire active waveguides. *Nano Lett.* **10**, 2251–2256 (2010).
43. L. K. van Vugt, B. Piccione, R. Agarwal, Incorporating polaritonic effects in semiconductor nanowire waveguide dispersion. *Appl. Phys. Lett.* **97**, 061115 (2010).
44. Y. L. Niu, Q. Peng, C. Deng, X. Gao, Z. Shuai, Theory of excited state decays and optical spectra: Application to polyatomic molecules. *J. Phys. Chem. A* **114**, 7817–7831 (2010).
45. Q. Peng, Y. Yi, Z. Shuai, J. Shao, Excited state radiationless decay process with Duschinsky rotation effect: Formalism and implementation. *J. Chem. Phys.* **126**, 114302 (2007).
46. Z. Shuai, Q. Peng, Excited states structure and processes: Understanding organic light-emitting diodes at the molecular level. *Phys. Rep.* **537**, 123–156 (2014).
47. Q. Bao, B. M. Goh, B. Yan, T. Yu, Z. Shen, K. P. Loh, Polarized emission and optical waveguide in crystalline perylene diimide microwires. *Adv. Mater.* **22**, 3661–3666 (2010).

48. D. O'Carroll, G. Redmond, Highly anisotropic luminescence from poly(9,9-dioctylfluorene) nanowires doped with orientationally ordered β-phase polymer chains. *Chem. Mater.* **20**, 6501–6508 (2008).
49. C. Quarti, D. Fazzi, M. Del Zoppo, A computational investigation on singlet and triplet exciton couplings in acene molecular crystals. *Phys. Chem. Chem. Phys.* **13**, 18615–18625 (2011).

Acknowledgments: We thank J. Huang (Northwestern University) and C.-L. Zou (Yale University) for helpful discussions. **Funding:** This work was supported by the Ministry of Science and Technology of China (grant nos. 2017YFA0204502 and 2015CB932404), the National Natural Science Foundation of China (grants nos. 21533013, 21790364, and 21421063), and the Strategic Priority Research Program of the Chinese Academy of Sciences (grants nos. XDB12020300 and XDB01020200). **Author contributions:** Y.S.Z. conceived the original concept and supervised the project. Q.H.C. and Y.S.Z. designed the experiments. Q.H.C. prepared the materials and devices. Q.H.C., Y.Y., and C.W. performed the optical measurements. Y.L., Q.P., Y.J., and Z.S. contributed to theoretical model. Q.H.C., Y.L., C.S., J.Y., and Y.S.Z. analyzed the data and wrote the paper. All authors discussed the results and commented on the manuscript. **Competing interests:** The authors declare that they have no competing interests. **Data and materials availability:** All data needed to evaluate the conclusions in the paper are present in the paper and/or the Supplementary Materials. Additional data related to this paper may be requested from the authors.

Submitted 18 September 2017
Accepted 7 February 2018
Published 16 March 2018
10.1126/sciadv.aap9861

Citation: Q. H. Cui, Q. Peng, Y. Luo, Y. Jiang, Y. Yan, C. Wei, Z. Shuai, C. Sun, J. Yao, Y. S. Zhao, Asymmetric photon transport in organic semiconductor nanowires through electrically controlled exciton diffusion. *Sci. Adv.* **4**, eaap9861 (2018).